ADVANCED QUANTUM TECHNOLOGIES
www.advquantumtech.com

Violation of No-Signaling on a Public Quantum Computer

Tomasz Rybotycki, Tomasz Białecki, Josep Batle, and Adam Bednorz**

No-signaling is a consequence of the no-communication theorem that states that bipartite systems cannot transfer information unless a communication channel exists. It is also a by-product of the assumptions of Bell theorem about quantum nonlocality. No-signaling is tested in bipartite systems of qubits from IBM Quantum devices in extremely large statistics, resulting in significant violations. Although the time and space scales of IBM Quantum cannot in principle rule out subluminal communications, there is no obvious physical mechanism leading to signaling. Such signaling is not universal in the relativistic but in a contextual sense. It assumes only lack of interaction between remote parts of the device. The violation is at similar level as observed in the Bell tests. It is therefore mandatory to check possible technical imperfections that may cause the violation and to repeat the loophole-free Bell test at much larger statistics, in order to rule out signaling definitively at strict space-like conditions.

1. Introduction

Quantum mechanics violates classical local realism, i.e., a counterfactual definite local hidden variable model generating measurement results.[1] It is shown by a Bell test,[2] i.e., violation of a certain inequality, usually Clasuer–Horne–Shimony–Holt (CHSH)[3] or Clauser–Horne,[4,5] which requires at least two separated observers, each performing randomly chosen measurements. The important assumption of local realism is the lack of communication between them, i.e., one party does not know the choice of the other one before accomplishing its own measurement. This assumption cannot be verified per se, but its consequences can. The most prominent effect that can be tested is no-signaling, that is the result of the measurement of one party cannot depend on the choice of the other one. Note that it applies to single-party measurements, while two-party correlations can depend on both choices, which is the essence of the Bell test. The violation of Bell-type inequalities is a proof of entanglement only when the no-communication assumption is valid. The other way round, if no-signaling fails, so fails no-communication, and the Bell violation of local realism is meaningless. Since passing the Bell test is the ultimate proof of entanglement and rejection of local realism, it should be accompanied by a verified no-signaling test.

Experimental Bell tests have a long history of closing detection and communication loopholes.[6–9] Detection loophole means that the measurement is in fact trichotomic, not dichotomic, common in early optical experiments when the low efficiency of photodetectors lead to high percentage of lost photons, assigned to a third outcome, and causing the whole event to be disregarded, or assigned to the other two. One can make a postelection, restricting the statistical events to both photons detected. To maintain the Bell conclusion, fair sampling was assumed, i.e., the counted fraction is representative and not used to invent yet another local hidden variable model.[10–13] In other implementations, the ones using superconductors in the form of either atoms or ions, it is never a problem. That's because the outcome is always dichotomic,[14–17] although auxiliary photons are sometimes preselected, i.e. one takes into account only cases when these photons are detected. In contrast to postselection, preselection is fully compatible with the Bell test, only lowering the overall statistics. Recent Bell experiments,[18,19] even photonic, have the detection loophole closed. However, not all of them do.[20–22]

The lack of communication can be in principle ruled out by setting the observers, their choices and measurements, within

T. Rybotycki
Systems Research Institute
Polish Academy of Sciences
6 Newelska Street, Warsaw PL01-447, Poland

T. Rybotycki
Nicolaus Copernicus Astronomical Center
Polish Academy of Sciences
18 Bartycka Street, Warsaw PL00-716, Poland

T. Rybotycki
Center of Excellence in Artificial Intelligence
AGH University
30 Mickiewicza Lane, Cracow PL30-059, Poland

T. Białecki, A. Bednorz
Faculty of Physics
University of Warsaw
ul. Pasteura 5, Warsaw PL02-093, Poland
E-mail: Adam.Bednorz@fuw.edu.pl

J. Batle
Departament de Física and Institut d'Aplicacions Computacionals de Codi Comunitari (IAC3)
Campus UIB, Palma de Mallorca, Balearic Islands E-07122, Spain
E-mail: jbv276@uib.es

J. Batle
CRISP – Centre de Recerca Independent de sa Pobla
sa Pobla, Balearic Islands E-07420, Spain

The ORCID identification number(s) for the author(s) of this article can be found under https://doi.org/10.1002/qute.202400661

DOI: 10.1002/qute.202400661

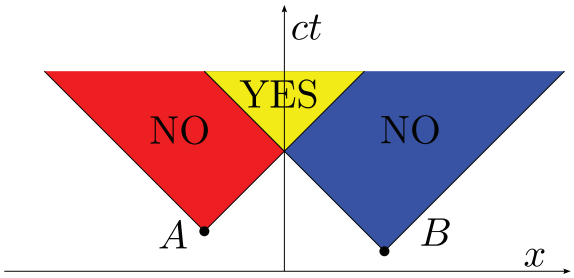

Figure 1. Depiction of signaling (YES) and no-signaling regions (NO) in spacetime, here reduced to a single spatial dimension x, time t and speed of light c. The choices of A and B marked by black points are the apexes starting the forward causal light cones (light triangles). Signaling only from A (B) is limited by relativistic causality axioms to the red (blue) region while the yellow part can receive signals from both parties. The remaining white region neither receives signals from A nor B. In the loophole-free Bell test, it is critical to accomplish the measurement within red and blue regions, for A and B observers, respectively.

a spatiotemporal framework. It is commonly assumed that the speed of light is the maximal speed of information transfer, but one has to remember that it does not simply follow from any, other than free, fundamental relativistic quantum field theory, because it is a non-perturbative claim.[23] It can be treated as an axiom, consistent with the general expectation of relativistic invariance of fundamental laws.[24,25]

To close the communication loophole, relying on the above axiom, the experimental setup requires sufficient spatial separation between observers so that the accomplished readout must lie outside the forward causal light cone created by the choice of the measurement of the other party, **Figure 1**. Although it is compelling from the relativistic point of view, one can still check no-signaling. Certainly, if the axiom is valid, as commonly expected, the test should be passed. On the other hand, one can treat no-signaling as a confirmation, of rather lack of falsification, of relativity as regards communication limit. In the recent loophole-free experiments,[26–30] no-signaling is routinely checked. Unfortunately, due to relatively small statistics, the present state is inconclusive.[31] A moderate violation of no-signaling occurs in the tests but has never been checked more accurately.[32,33] A collection of various Bell-type tests[34] revealed even more troubles.[35] In the first test on superconductors,[17] no-signaling was violated by 70 standard deviations at extremely large number of trials ($\sim 34 \cdot 10^6$). This was attributed to measurement crosstalk at small distances. The recent loophole-free test[30] violates no-signaling at the p-value (the probability to observe the experimental data given the null hypothesis holds) of 2%[36] at $\sim$250000 trials per a pair of choices. Both violations are of the same order so it is tempting to ask what if one rerun the latter test with a much larger number of trials.[37]

Regarding relativity, it is treated as the ultimate bound on communication, although the physical description of the loophole-free setups is not directly relativistically covariant (light in the fibers/waveguide travels at about the phase velocity 2/3 of the vacuum speed, due to an immobile medium) However, even at small distances and long times, any communication needs a reasonable physical origin, an appropriate propagating interaction. In this case violation of no-signaling is helpful in detection of unspecified communication channels and its analysis can reveal possible interaction mechanism. One can also ask what kind and amount of signaling can be used to invent a local realistic model.[38] No-signaling can be tested also without assuming identical distributions.[39] We emphasize that no-signaling at non-relativistic scales demonstrates valid connection structure, tests possible remote interactions and allows identifying and/or eliminate erroneous physical components. The assumption of lack of remote interactions will be here called contextual no-signaling, to distinguish it from the universal relativistic bounds. It is still an important check of the experimental setup. For example, in refs. [40, 41] the no-signaling holds even within the light cone. At non-relativistic scales no-signaling is rather a property of the physical separation of the parties that cannot affect each other, leading formally to commutation between the action at one party and the detection at the other one.[42–45]

Publicly available quantum computers, such as IBM Quantum, offer the real qubits (basic two-level systems, realized on transmons - superconducting Josephson junction shunted with capacitance)[46,47] and gates (operation on a single qubit or a pair of them, realized by microwave pulses),[48–55] Such a computer is expected to realize relatively faithfully the prepared sequences of operations, although they are often noisy, and cause some crosstalk. Nevertheless, the errors are quite well identified, by thermal noise, leakage to excited states or to the nearest neighbors. More complicated technical imperfections are expected to be so negligible that they can be disregarded. One can also run Bell-type tests on such computers,[56–59] although the communication loophole in the relativistic sense remains open, due to small distances compared to the gate and measurement pulse times. To prevent memory effects, e.g. the dependence on the preceding run, one can shuffle the settings. Violation of no-signaling is therefore a signature serious technical malfunction but not necessarily superluminal interaction. In any case, a quite sophisticated interaction model is needed to explain it, far beyond the current grid of qubit connections.

In this work, we present the results of tests of no-signaling on IBM Quantum devices. They are composed of heavy hexagonal 127-qubit grids where each qubit is directly connected with one, two, or three other qubits. The connections allow realizing two-qubit gates to create entanglement and in principle to perform multi-qubit operations transpiled into a sequence of gates native to the device. Transpiling is a decomposition of operations on large sets of qubit into a sequence microwave pulses focused on single qubit or pairs of them. In the IBM topology, only spatially adjacent qubits can interact, but a sequence of two-qubit gates allows, in principle, any multi-qubit operation, at the price of error related to the complexity and length of the sequence.

We performed three types of experiments, testing signaling between next neighbors and fourth neighbors (parties separated by a chain of 3 other qubits). The nearest, direct neighbors may affect each other by the connection. The experiments are:

1) Bell test on next neighbors,
2) idle test (i.e. local Bell measurements without any entanglement) on next neighbors,
3) idle test on fourth neighbors.

IBM Quantum allows to run tests simultaneously on several pairs of qubits, limited by possible paths overlapping. We have

shuffled randomly the circuits with different settings to excluded potential memory effects. We have found that: 1) Bell inequality is violated in the majority of pairs in the test a), 2) no-signaling is violated in all a-b) tests, but it is most prominent if a qubit interlevel frequencies are similar, but still of lower order than Bell violation, 3) violation of no-signaling occurs also in c), but it is much smaller and sometimes requires larger statistics to increase confidence in it.

In each test, we have found significant violations, at p-value below the threshold equivalent to 5 standard deviations, with additional borderline cases, that may become significant if continuing data collection.

The paper is organized as follows. We start with the description of the circuits implemented on IBM Quantum for each test. Next, we present the results of both Bell and no-signaling tests. Then we explain the commonly suspected origins of signaling which fail to reproduce the observed violations. Finally, some conclusions are drawn and discussed. Additional technical details are given in the Appendix.

2. Bell and No-Signaling Tests

Implementation of Bell and no-signaling tests on IBM Quantum relies on the grid of qubits, two-level systems with basis states $|0\rangle$ and $|1\rangle$, in energy eigenspace, differing by the energy $\hbar\omega$. Here $f = \omega/2\pi$ is the qubit frequency. Those are manipulated by the quantum gates, operations on single or pairs of the qubits. The states can be either pure $\rho = |\psi\rangle\langle\psi|$ or mixed, i.e. a convex normalized combination of pure states. Single qubit states are often represented as vectors on the Bloch ball $\rho = (I + \boldsymbol{\sigma}\cdot\boldsymbol{\nu})/2$ for the set of Pauli matrices σ_k, $k = 1, 2, 3$ and vector $\boldsymbol{\nu} = (\nu_1, \nu_2, \nu_3)$ such that $|\boldsymbol{\nu}| \leq 1$.

A microwave pulse tuned to the qubit frequency allows one to apply the parametrically controlled gates. The native single qubit gate we use is the $\pi/2$ rotation on the Bloch sphere about the axis (1,0,0)

$$S = \sqrt{X} = (1 - i\sigma_1)/\sqrt{2} = \frac{1}{\sqrt{2}}\begin{pmatrix} 1 & -i \\ -i & 1 \end{pmatrix} \tag{1}$$

in the computational basis. The auxiliary θ-rotation about (0,0,1) axis, $Z(\theta)$, is a virtual operation,

$$Z_\theta = \begin{pmatrix} e^{-i\theta/2} & 0 \\ 0 & e^{i\theta/2} \end{pmatrix} \tag{2}$$

realized by a phase shift of the next gate, i.e.

$$S_\theta = Z_\theta^\dagger S Z_\theta = \frac{1}{\sqrt{2}}\begin{pmatrix} 1 & -ie^{i\theta} \\ -ie^{-i\theta} & 1 \end{pmatrix} \tag{3}$$

The gate S_θ is essentially realized by taking the pulse from (1) with a phase offset θ, mixing sine and cosine components. The offset changes the rotation axis on the equator of the Bloch sphere. It does not change the amplitude of the pulse. Moreover, the pulse is based on a wave of a constant frequency (local oscillator). Even if qubits have similar but not identical frequencies, the relative phases of different local oscillators are random. In addition, there is a two-qubit $CNOT_\downarrow$ gate, operating as

$$|00\rangle\langle 00| + |01\rangle\langle 01| + |11\rangle\langle 10| + |10\rangle\langle 11| \tag{4}$$

where for $|ab\rangle$ the control qubit state is a (depicted as •) and target qubit state is b (depicted as $\oplus$ in **Figure 2**). The IBM Quantum devices use Echoed Crossed Resonance (ECR) gate, instead of $CNOT$. This is not a significant issue, because one can transpile the latter by using the former and some additional single-qubit gates (see Appendix A).

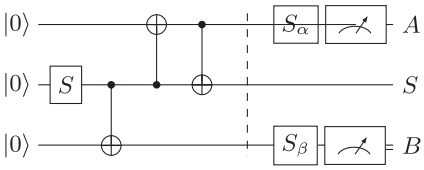

Figure 2. Standard realization of the CHSH test on IBM Quantum for next neighbors in the test a). The gate S creates a superposition of $|0\rangle$ and $|1\rangle$ states on the source qubits S, entangled with the neighbor B by the $CNOT$ gate, and swapped by a pair of $CNOT$s to the other neighbor A. The final measurements are the sequences of S and $S_{\alpha/\beta}$ gates (1) and (3). In the tests b,c), the entangling part left of the vertical dashed barrier are absent.

For the test a), we create an entangled state, applying S gate to the state $|0\rangle$ of the source qubit, to get $\sqrt{2}|\psi_0\rangle = |0\rangle - i|1\rangle$ and after the $CNOT$ gate $\sqrt{2}CNOT|\psi_0 0\rangle = |00\rangle - i|11\rangle$. We swap one of qubits with the neighbor by $CNOT_\downarrow CNOT_\uparrow |0\phi\rangle = |\phi 0\rangle$, which holds for an arbitrary $|\phi\rangle$.

The final Bell measurements A_a and B_b are performed by $SZ_\alpha \equiv S_\alpha$ on qubits A and S_β on qubit B, with the Bell angles $\alpha = 0, \pi/2$ for settings $a = 0, 1$ and $\beta = -\pi/4, \pi/4$ for settings $b = 0, 1$, respectively. The readout is projective measurement, meaning that it maps the states for the values of observables A or B: $|0\rangle \to +1$ and $|1\rangle \to -1$ (we shall abbreviate $\pm 1 \to \pm$).

In the ideal case $\langle A\rangle = \langle B\rangle = 0$ while $\langle AB\rangle = -\sin(\alpha + \beta)$, for the average/correlation defined $\langle x\rangle_{ab} = \sum_x x P_{ab}(x)$ with the $P_{ab}(x)$ being the probability of the outcome x for settings ab.

The whole circuit is depicted in Figure 2. We can construct CHSH inequality

$$C = \sum_{ab} s_{ab}\langle AB\rangle_{ab} \leq 2,$$

$$s_{ab} = \begin{cases} +1 & \text{for } a = b = 0 \\ -1 & \text{otherwise} \end{cases} \tag{5}$$

which is violated at $2\sqrt{2} \simeq 2.828$.

The other tests do not contain the entangling part, just measurements, i.e. operations $S_{\alpha/\beta}$, with the same values $\alpha_{0,1} = 0, \pi/2$ and $\beta_{0,1} = -\pi/4, +\pi/4$ and the same or larger distances between A and B, as described in **Table 1**.

No-signaling is the condition to be satisfied both in classical and quantum mechanics. On the quantum level, if the operator of the party A commutes with the other party, $AB = BA$, then A cannot affect B, and viceversa. It is the basic relativistic axiom.[24] However, the contextual assumption remains in general.

The contextual no-signaling test is performed as follows. In

Table 1. Differences among the tests a-c regarding entanglement and distance.

test	entanglement	$A-B$ distance
a)	yes	2
b)	no	2
c)	no	4

each of a-c) tests, we measure the probability $P_{ab}(AB)$, i.e. how often the pair of values AB are measured for a given pair of settings ab. Then we define single-party probability $P(A*) = \sum_B P(AB)$, $P(*\ B) = \sum_A P(AB)$. No-signaling holds if

$$\delta P_{a*} = P_{a0}(+*) - P_{a1}(+*),$$
$$\delta P_{*b} = P_{0b}(*+) - P_{1b}(*+) \tag{6}$$

are both equal to 0. For an ideal implementation $P(A*) = P(*\ B) = 1/2$ regardless of AB and ab. For transmons, it is not necessary to correct the above equation by the detection efficiency, which is required for photons.[60] Due to finite statistics, the probabilities are taken from the actual counts, i.e. $P(x) = N_x/N$, where N_x is the number for trials giving the outcome x. The possible probability error can be quantified, assuming independence of the trials. For an equal number of trials N, we have

$$N\sigma^2 = N\langle(\delta C)^2\rangle = \sum_{ab}(1 - \langle AB\rangle^2_{ab}),$$
$$N\sigma^2_{a*} = N\langle(\delta P_{a*})^2\rangle = \sum_b P_{ab}(+*)P_{ab}(-*),$$
$$N\sigma^2_{*b} = N\langle(\delta P_{*b})^2\rangle = \sum_a P_{ab}(*+)P_{ab}(*-) \tag{7}$$

where δC is the statistical deviation from (5) calculated for the actual statistics. The error is crucial to identify significance of the potential violation of Bell inequality or no-signaling. In addition, one can express the significance in terms of $p-$value, i.e. the probability that the local realism or no-signaling hypothesis holds. It is calculated as the double tail of the Gaussian probability distribution (which is a limiting distribution of a sum of many independent random variables) centered at 0, with the standard deviation σ, i.e. events below $-|z|$ and above $+|z|$ for the z score corresponding to the actually observed value,

$$p(z) = 2\int_z^\infty e^{-z^2/2\sigma^2}/\sqrt{2\pi\sigma^2} = \mathrm{erfc}\,(z/\sqrt{2}\sigma) \tag{8}$$

The actual p-value is taken from the above formula, but multiplied by the number of possible tests, also known as Bonferroni corrections or look-elsewhere effect.[61,62]

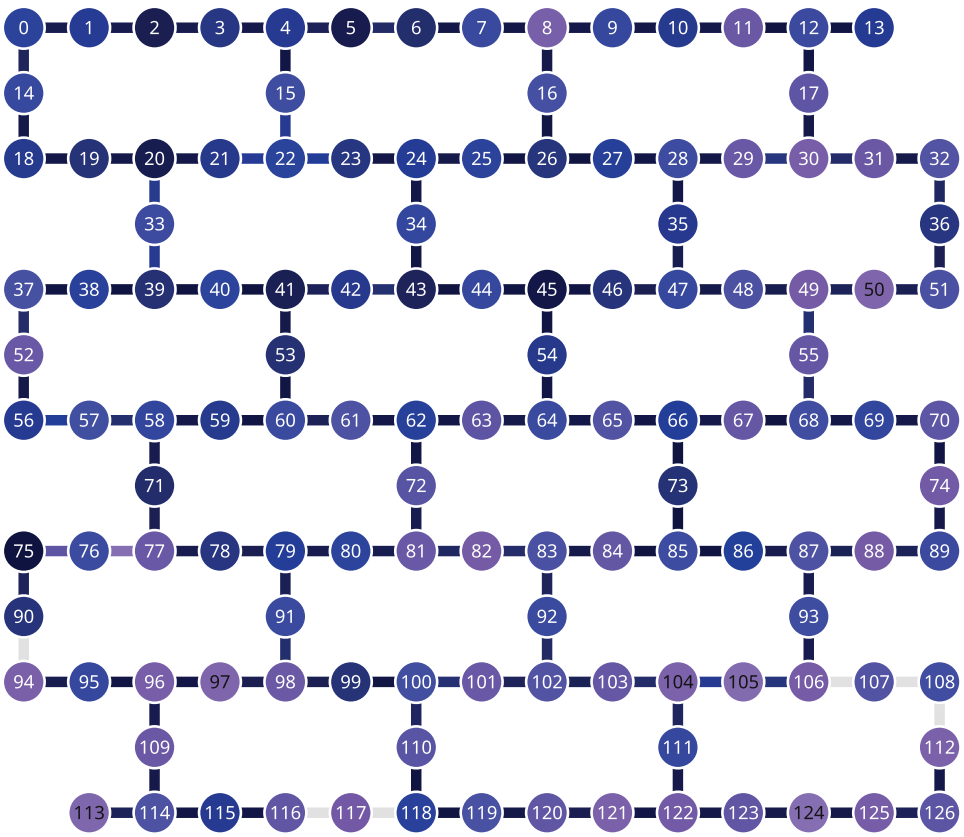

Figure 3. Topology of the qubit grid of IBM Quantum devices in Eagle generation, `ibm_sherbrooke`, `ibm_brisbane`, `ibm_kyoto`, `ibm_kyiv`. Here the circles represent qubits, bars connections for two-qubit gates. The grid is actually hexagonal.

Table 2. Results of the test a) and b) for `ibm_kyoto`, qubits A and B as specified, with the source qubits S (middle). Here, all σ and δP are in units 10^{-4} while $f_{A-B} = f_A - f_B$ is the frequency difference between qubit A and B in MHz. The error $\sigma_{a*}, \sigma_{*b} \simeq 1.3 \cdot 10^{-4}$. We have highlighted in bold the strongest violations of no-signaling.

$A-S-B$	a)	$\mathcal{C}$	σ	δP_{0*}	δP_{1*}	δP_{*0}	δP_{*1}	b)	δP_{0*}	δP_{1*}	δP_{*0}	δP_{*1}	f_{A-B}
55-68-67		2.25	3.0	**103**	**281**	**104**	**−64.2**		**−93.9**	**−227**	**−185**	**−87.6**	0.77
34-43-44		2.4	3.0	**70.8**	**63.3**	**85**	**84.3**		**26.4**	**−112**	**−59**	**19.1**	−4.2
29-30-31		1.84	3.2	**−12.6**	6.32	−0.617	**−20.3**		**−25**	**88.2**	**89**	**−23.1**	−5.5
101-102-103		2.15	3.0	**−50.1**	**−76**	**−63.7**	**−28.3**		**−73.2**	**10.2**	**62.7**	**−71.9**	6.8
7-8-9		1.6	3.0	**−40.9**	**−12.7**	**−13.9**	**−47.1**		4.55	−3.02	−2.75	3.75	8.2
74-89-88		2.26	2.8	2	−2.78	−0.305	3.11		−1.87	**−14.2**	7.85	**34.4**	−9.3
94-95-96		2.14	3.0	**8.74**	6.7	3.98	3.28		−7.87	−5.25	−4.35	**−17.6**	15
25-26-27		2.37	3.0	2.37	−6.63	−1.91	**8.89**		7.83	**10.5**	1.53	**16.3**	15
63-62-72		2.45	2.8	0.569	−0.013	−1.11	0.904		−3.24	2.93	4.9	−4.48	17
38-39-40		2.34	2.8	0.0717	−7.03	**−8.67**	**−9.78**		−0.827	1.72	0.814	4.08	−17
58-59-60		2.28	3.0	1.8	−1.53	−1.67	5.53		**14**	2.87	5.38	**18.6**	−20
21-22-23		1.59	3.4	2.92	−1.69	−0.678	3.76		−0.112	5.26	7.78	−0.222	21
80-79-91		2.19	3.0	0.352	1.55	4.17	2.34		1.94	−0.324	0.962	−0.988	−26

3. Results

IBM Quantum allows running experiments in the single units called jobs. Each job consists of a sequence of circuits, which can be different in general. Each circuit corresponds to an individual experiment run, as specified in the previous section, i.e., a sequence of gates ending with measurements. The standard time for a single run is 250 microseconds. Each sequence of circuits is repeated by the number of shots, specified in the job description.

We have run tests a-b) on the same sets of qubits, on Eagle generation `ibm_sherbrooke`, `ibm_brisbane` and `ibm_kyoto`, with 60 jobs, 20000 shots each, and on `ibm_kyiv` with 58 and 60 jobs, 7500 shots for test a) and b) respectively. The limited number of shots and jobs on `ibm_kyiv` was due to a slower circuit executions. We had 25 repetitions for each choice configuration ab, all randomly shuffled, giving the total number of 100 circuits per job. We tested simultaneously several non-overlapping pairs of next-neighbor qubits (topology of IBM Quantum devices is depicted in **Figure 3**). It gives the total number of trials equal to $3 \cdot 10^7$ (except $\sim 10^7$ for `ibm_kyiv`). The tests c) on the same devices, have been run with the same number of jobs (60 for `emph_kyiv`), shots and repetitions, except for `ibm_sherbrooke`, where the number of jobs was 240. The results of Bell and no-signaling tests are given in **Tables 2–9**. The standard deviation in almost all tests is roughly the same, $1.3 \cdot 10^{-4}$, except for c) on `ibm_sherbrooke`, where it was $6.4 \cdot 10^{-5}$. The jobs were run in August 2024, expect for b) and c) on `ibm_kyiv`, which was done in September 2024. Each job takes about 530 seconds. The total run time was several hours, except c) on `ibm_sherbrooke`, which took about 3 days. During the test, the devices underwent routine calibrations, which shouldn't affect the experiment, as the test is linear. In particular, the qubit drive frequencies may vary at the relative level $\sim 10^{-6}$.

It turns out that the majority of tests a) confirm violation of Bell-CHSH inequality, but a-b) also often violate no-signaling. The violation of no-signaling is the strongest when the frequencies of A and B are similar, but it still happens in some cases with large frequency difference (e.g. 80-82 on `ibm_sherbrooke`

Table 3. Results of the test a) and b) for `ibm_brisbane`, notation as in Table 2.

$A-S-B$	a)	$\mathcal{C}$	σ	δP_{0*}	δP_{1*}	δP_{*0}	δP_{*1}	b)	δP_{0*}	δP_{1*}	δP_{*0}	δP_{*1}	f_{A-B}
1-2-3		1.68	3.2	−4.21	0.275	**−10.6**	2.34		−1.09	−0.531	−0.24	−0.709	−60
7-8-9		2.15	2.8	0.072	**21.6**	**19.8**	4.54		−1.32	**17.4**	**9.61**	6.68	−20
11-12-13		2.06	3.2	**10.4**	−2.88	−3.08	0.688		−0.663	−2.76	−0.184	0.108	−34
39-40-41		2.38	2.8	−2.44	−1.87	−3.14	−3.63		**9.75**	**9.53**	7.08	5.34	−18
44-45-46		2.31	3.0	−7.11	0.813	**8.66**	0.149		−3.55	0.577	0.951	0.882	96
67-68-69		1.68	3.2	**−55.7**	**38.5**	**17**	**−75.9**		**−37.6**	**−14.6**	**−46**	**−47.5**	−3.7
79-80-81		1.61	3.2	4.46	−2.55	7.57	−3.06		−1.62	−0.248	1.64	−2.14	−67
83-84-85		2.39	3.0	**−8.1**	−0.238	0.447	−1		−2.17	1.65	−1.53	1.08	−310
95-96-97		2.18	3.0	−6.06	−1.76	1.54	−6.21		−2.48	3.84	6.44	−1.96	23
106-107-108		2.01	3.3	−0.104	−0.445	−6.61	1.63		−0.55	2.37	−1.05	−3.26	−180
113-114-115		1.94	3.3	**78.8**	**114**	**94**	**56.6**		**32.5**	71.4	**58.9**	**28**	4
122-123-124		2.44	2.8	**−10.6**	**−31.8**	**−25.2**	−2.62		−6.79	**54**	**24.8**	**−14.6**	−12

Table 4. Results of the test a) and b) for `ibm_sherbrooke`, notation as in Table 2.

$A-S-B$	a)	$\mathcal{C}$	σ	δP_{0*}	δP_{1*}	δP_{*0}	δP_{*1}	b)	δP_{0*}	δP_{1*}	δP_{*0}	δP_{*1}	f_{A-B}
4-5-6		2.06	3.2	2.66	−0.795	−6.22	2.16		2.38	1.02	0.362	−2.15	−110
11-12-13		2.25	3.0	1.6	0.38	1.35	0.881		−2.08	3.33	−1.39	−1.66	190
21-22-23		1.57	3.4	**13.9**	**14.4**	**9.63**	**13**		−6.15	4.48	**8.44**	−6.7	16
28-29-30		2.23	3.0	**−22.5**	6.73	2.41	0.217		0.156	−0.5	0.324	0.338	51
37-38-39		2.41	2.8	**8.58**	**8.94**	3.52	−0.321		−1.71	**−11.1**	**−10.1**	0.926	20
43-44-45		2.54	2.8	4.65	**−82.3**	−4.03	**87.2**		**48.1**	**56**	**59.2**	52.7	−7.7
47-48-49		2.6	2.8	−4.1	**−12.7**	**−18.5**	**−14.5**		−5.13	**−11.6**	−7.11	−7.94	−16
60-61-62		2.31	3.0	0.306	−1.53	−1.2	−0.15		0.958	−0.0307	−1.05	−1.51	−99
80-81-82		1.24	3.4	21	**−8.86**	0.435	−0.775		−0.627	−0.605	−2.56	1.93	230
94-95-96		2.06	3.0	1.34	−1.12	1.43	−0.204		0.021	1.79	1.52	2.29	−130
102-103-104		2.55	2.8	**133**	**198**	**101**	**29.9**		**−12.7**	**152**	**159**	**−12.3**	2.8
117-118-119		2.53	2.8	**313**	**510**	**306**	**103**		**−295**	**249**	**242**	**−308**	0.43
123-124-125		2.49	2.8	−2.02	0.874	−1.38	−1.02		1.46	2.27	−1.22	0.827	−160

Table 5. Results of the test a) and b) for `ibm_kyiv`, notation as in Table 2, except error. The error σ_{a*}, $\sigma_{*b} \simeq 2.14 \cdot 10^{-4}$, and $2.1 \cdot 10^{-4}$, in test a) and b) respectively.

$A-S-B$	a)	$\mathcal{C}$	σ	δP_{0*}	δP_{1*}	δP_{*0}	δP_{*1}	b)	δP_{0*}	δP_{1*}	δP_{*0}	δP_{*1}	f_{A-B}
11-12-13		2.36	4.8	**−40.7**	**109**	0.0432	**−145**		**−115**	**−61.9**	**−70**	**−109**	−1.8
80-81-82		1.82	5.4	**123**	**184**	**184**	**106**		**−17.2**	**140**	**167**	**−32.2**	−1.8
24-25-26		2.39	4.8	**−166**	**−85.2**	**−191**	**−272**		**−91.4**	**186**	**197**	**−82.4**	−2.6
31-32-36		2.33	5.0	**22.5**	**−23.2**	**17.1**	**65.5**		**14.3**	**−51.5**	**−42.8**	**12.9**	5
92-102-101		2.6	4.6	**−12.7**	**−66.6**	−7.44	**53.3**		3.34	**61.3**	**60.6**	−0.008	5.2
9-8-16		2.16	5.0	−4.21	−12.2	−8.86	2.11		**−21.3**	**22.6**	**28.2**	**−20.6**	5.8
38-39-40		2.21	5.0	−5.75	**−34.9**	−1.25	**24.6**		**−69.2**	**21.8**	**19.2**	**−81.1**	−5.8
77-78-79		2.17	5.0	**−30.6**	−12.5	**−49.3**	**−71.6**		**−42.7**	**25.2**	**26**	**−49.7**	5.9
54-64-63		2.5	4.8	**−63.1**	**−17.4**	**−78**	**−111**		**−58.3**	**−70.6**	**−63.8**	**−49.6**	−6.1
123-124-125		2.13	5.0	**58.7**	**64.7**	**67**	**64.9**		**37.7**	2.48	5.58	**43.9**	−6.5
84-85-86		1.61	5.0	6.63	8.89	9.27	4.54		−10.5	**20.3**	**13.5**	−6.92	−6.8
119-120-121		2.07	5.2	**46.9**	**36.6**	**45.7**	**57.2**		**−26.3**	**31.3**	**31.4**	**−19.1**	−9.6
15-22-21		2.41	4.8	−1.11	2.02	−2.56	−3.84		−8.84	−3.21	−6.3	**−20.5**	11

and 44-46 on `ibm_brisbane` with differences 230 and 96 MHz, respectively). In all tests c) there are also pairs violating no-signaling, but the violation is smaller. In any case, it still seems larger at small frequency difference.

We have additionally analyzed the extreme case of test c), `ibm_sherbrooke` pair 49-66, checking the probability, **Table 10**, and results of δP for individual jobs, **Figure 4**. No accidental violation has been found, although the violation may get

Table 6. Results of the test c) for `ibm_kyoto`, notation as in Table 2.

$A-B$	δP_{0*}	δP_{1*}	δP_{*0}	δP_{*1}	f_{A-B}
11-31	2.73	0.531	1.03	−1.08	−0.06
77-81	−3.43	1.46	−0.557	−1.12	0.073
42-59	1.35	−0.644	0.909	−1.69	−1.6
116-120	**22.3**	**23.3**	**−22.8**	**24.4**	3.7
68-85	**−36.8**	−0.803	**19.6**	−3.17	8.8
15-33	**−16.7**	**−9.9**	5.57	−0.193	5.7
84-103	−3.09	**9.67**	−1.39	**17.6**	−6.3
97-113	**10**	**14.4**	**35.7**	−5.35	−7.1

Table 7. Results of the test c) for `ibm_brisbane`, notation as in Table 2.

$A-B$	δP_{0*}	δP_{1*}	δP_{*0}	δP_{*1}	f_{A-B}
41-62	−0.425	−0.0373	−0.935	0.216	0.32
76-95	2.2	0.705	1.12	1.81	−1.5
15-25	−2.18	−0.307	0.982	1.38	2.8
7-11	3.52	−2.21	−1.65	−0.457	−4.8
28-45	**−11.4**	**−25.5**	**20.3**	−2.42	−5
82-86	−0.231	−0.626	0.86	0.168	−5.2
111-125	−0.417	1.7	−4.02	−0.802	−6
100-116	**−10.6**	−1.02	**9.64**	**−10.9**	−7.4

Table 8. Results of the test c) for `ibm_sherbrooke`, notation as in Table 2, except that here $\sigma_{a*}, \sigma_{*b} \simeq 6.4 \cdot 10^{-5}$.

$A-B$	δP_{0*}	δP_{1*}	δP_{*0}	δP_{*1}	f_{A-B}
109-117	−0.284	0.59	−0.0604	−0.775	0.99
49-66	−3.36	3.29	1.86	**−5.89**	1.2
68-85	0.102	−0.244	−1.39	0.109	−4
92-99	−0.456	0.542	−0.705	−1.7	−4.7
34-40	0.293	0.81	0.421	−0.00325	5.2
27-46	2.22	−0.283	−0.376	−1.04	6.3
120-124	1.53	−1.51	−3.8	1.33	6.5
52-71	0.877	−0.484	0.247	0.665	8.6

Table 9. Results of the test c) for `ibm_kyiv`, notation as in Table 2, except that here $\sigma_{a*}, \sigma_{*b} \simeq 2.1 \cdot 10^{-4}$.

$A-B$	δP_{0*}	δP_{1*}	δP_{*0}	δP_{*1}	f_{A-B}
97-110	−3.38	−1.41	−0.692	−2.15	0.87
26-30	3.42	1.92	−0.00711	0.307	2.2
3-14	−0.0507	5.28	−3.34	−1.58	2.6
62-66	2.1	−3.9	−3.46	−2.37	−3.6
43-60	1.06	−0.298	1.51	−0.499	5.5
105-123	0.185	2.29	−3.87	3.44	9.3
18-39	**−32.3**	**26.1**	−8.65	1.48	10
6-10	2.88	−0.268	−1.15	−0.723	12

some drift over time. The $p-$value is $5.3 \cdot 10^{-17}$, taking into account estimating $127 \cdot 8$ possible pairs by the look elsewhere effect, compared to the agreed border at 5 standard deviations, $5.7 \cdot 10^{-7}$. The data and the scripts we used are publicly available.[63]

4. Analysis of Technical Imperfections

The observed violations of no-signaling are significant, but vary between different qubit pairs. It is tempting to seek for the origin in technical imperfections of IBM Quantum devices. It is known that frequency collisions lead to serious crosstalk, but usually due to two-qubit gates driven by the pulses of one qubit frequency applied to the other qubit.[64,65] Certainly the measurement times of > 1 microsecond compared to the distances of several cm allows communication in the relativistic sense. However, there are no obvious interactions responsible for it. The most natural ZZ crosstalk, i.e. the interaction diagonal in the energy basis of the set of qubits, does not help, as $S_{\alpha/\beta}$ pulses differ only by the phase offsets, not amplitudes. An error of an S gate is insufficient if the Z gate (phase shift) works correctly. It is the Z gate that must be erroneous, which means an error at the time of pulse preparation. The microwave pulse is formed by combining Arbitrary Waveform Generator (AWG), Local Oscillator (LO) generating continuous wave of the qubit frequency and in-phase/quadrature mixer (IQM), i.e., the device that combines signals of phase shifted by $\pi/2$,[66] see **Figure 5**. Normally, even if LO have similar frequencies, they are not exactly equal and the phases are not synchronized. Any phase shift is added to an individual LO phase so the effect on the other qubits is random.

Table 10. Probabilities for $P_{ab}(AB)$ for the test c) on `ibm_sherbrooke` pair $A-B: 49-66$.

ab	$P(++)$	$P(+-)$	$P(-+)$	$P(--)$	$P(+*)$	$P(*+)$
00	0.27779	0.22945	0.26979	0.22297	0.50724	0.54758
10	0.28060	0.23202	0.26679	0.22059	0.51262	0.54740
01	0.27800	0.22958	0.26975	0.22267	0.50758	0.54775
11	0.28092	0.23137	0.26742	0.22029	0.51229	0.54834

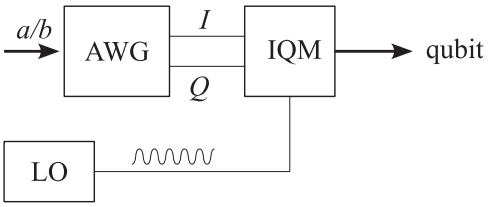

Figure 5. The signal flow from the choice a/b to the actual qubits drive pulse. The AWG creates a pulse amplitude with its in-phase I and quadrature Q component. The LO creates the continuous wave of the qubit drive frequency. The IQM combines the two waves into a single microwave pulse applied to the qubit.

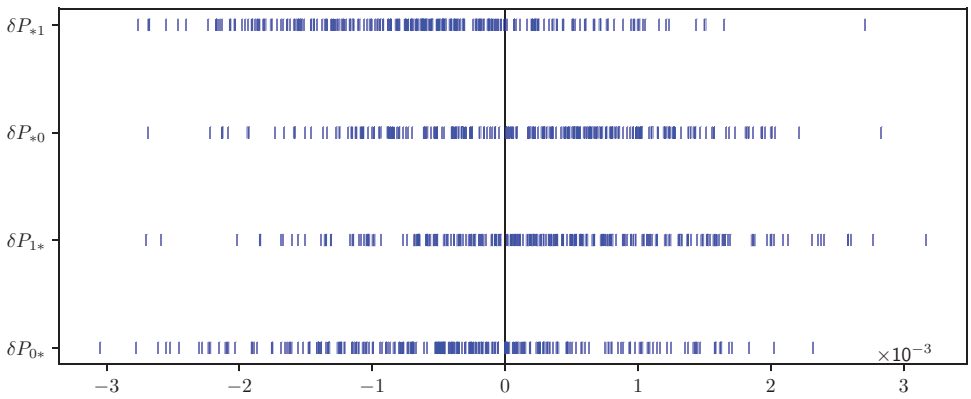

Figure 4. Signaling defined by Equation (6) calculated in the test c) on `ibm_sherbrooke` pair $A-B: 49-66$ for each individual job, i.e. each bar corresponds to the value calculated for a single job, out of 240.

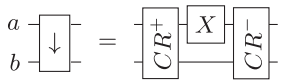

Figure A1. The notation of the *ECR* gate in the $ECR_{\downarrow}|ab\rangle$ convention.

Only if the phase shift is correlated with the pulse amplitude error, the subsequent *ZZ* crosstalk may cause signaling. We estimate the magnitude of direct *ZZ* coupling below the error of two level gates $\lesssim 1\%$, and any remote coupling, at the distances 2 or 4, as in our tests, is expected to be even smaller. On the other hand, amplitude error would lead to significant local error, i.e., much more significant change of the qubit directly controlled, not the other party, which we do not observe, see e.g. Table 10. An explanation by mid-circuits crosstalk[67] does not apply here as the qubits in question are not directly connected, and the measurements in our circuits occur after the last phase-shifted gates.

5. Discussion

We have checked Bell inequality and no-signaling on IBM Quantum devices. It turns out that although Bell violation is observed, there is also violation of no-signaling. The latter is significant and cannot be explained by a simple crosstalk. The level of the violation is similar to other superconducting experiments,[17,30] at very high statistics. It is urgent to resolve the origin of the violation. Other tests, possibly in different configuration or implementation, should be run. Also, the loophole-free Bell experiment[30] should be also rerun at a larger number of trials and various configurations (also idle, and with various sets of angles). It is certainly difficult to quantify the consequences that these errors may entail in more involved experiments, or how they propagate when global multi-qubit tasks are involved. Thus, a thorough further technical analysis to ascertain the exact source of errors is absolutely imperative for future endeavors.

Appendix A: Relation Between *CNOT* and *ECR* Gates

The IBM Quantum devices use the two-qubit *ECR* instead of *CNOT*,[50,51] but one can transpile the latter by the former, by adding single qubits gates. We shall use Pauli matrices in the computational basis,

$$X=\begin{pmatrix}0&1\\1&0\end{pmatrix},\ Y=\begin{pmatrix}0&-i\\i&0\end{pmatrix},\ Z=\begin{pmatrix}1&0\\0&-1\end{pmatrix},\ I=\begin{pmatrix}1&0\\0&1\end{pmatrix} \tag{A1}$$

We also denote two-qubit gates by ↓ and ↑, which mean the direction of the gate (it is not symmetric), i.e. $\langle a'b'|G_{\uparrow}|ab\rangle=\langle b'a'|G_{\downarrow}|ba\rangle$.

The *ECR* gate acts on the state $|ab\rangle$ as (**Figure A1**)

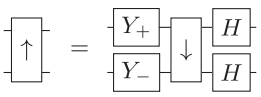

Figure A2. The $ECR_{\uparrow}$ gate expressed by the $ECR_{\downarrow}$.

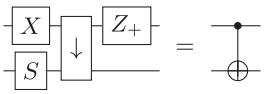

Figure A3. The $CNOT_{\downarrow}$ gate expressed by the $ECR_{\downarrow}$.

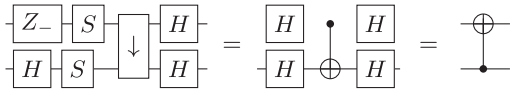

Figure A4. The $CNOT_{\uparrow}$ gate expressed by the $ECR_{\downarrow}$.

$$ECR_{\downarrow}=(XI-YX)/\sqrt{2}=CR^{-}(XI)CR^{+}=$$
$$\begin{pmatrix}0&X_{-}\\X_{+}&0\end{pmatrix}=\begin{pmatrix}0&0&1&i\\0&0&i&1\\1&-i&0&0\\-i&1&0&0\end{pmatrix}/\sqrt{2} \tag{A2}$$

in the $\{|00\rangle,|01\rangle,|10\rangle,|11\rangle$ basis, where the native gate is

$$S=X_{+}=X_{\pi/2}=(I-iX)/\sqrt{2}=\begin{pmatrix}1&-i\\-i&1\end{pmatrix}/\sqrt{2} \tag{A3}$$

and $X_{-}=X_{-\pi/2}=ZX_{+}Z$, with

$$CR^{\pm}=(ZX)_{\pm\pi/4} \tag{A4}$$

using the convention $V_{\theta}=\exp(-i\theta V/2)=\cos(\theta/2)-iV\sin(\theta/2)$ if $V^2=I$ or *II*. The gate is its inverse, i.e. $ECR_{\downarrow}ECR_{\downarrow}=II$.

Note that $Z_{\theta}=\exp(-i\theta Z/2)=\mathrm{diag}(e^{-i\theta/2},e^{i\theta/2})$ is a virtual gate adding essentially the phase shift to next gates. *ECR* gates can be reversed, i.e., for $a\leftrightarrow b$, (**Figure A2**)

$$ECR_{\uparrow}=(IX-XY)/\sqrt{2}=(HH)ECR_{\downarrow}(Y_{+}Y_{-}) \tag{A5}$$

denoting $V_{\pm}=V_{\pm\pi/2}$, Hadamard gate

$$H=(Z+X)/\sqrt{2}=Z_{+}SZ_{+}=\begin{pmatrix}1&1\\1&-1\end{pmatrix}/\sqrt{2} \tag{A6}$$

and $Z_{\pm}SZ_{\mp}=Y_{\pm}$, with $Y_{+}=HZ$ and $Y_{-}=ZH$.

The *CNOT* gate can be expressed by *ECR* (**Figure A3**)

$$CNOT_{\downarrow}=(II+ZI+IX-ZX)/2=$$
$$\begin{pmatrix}I&0\\0&X\end{pmatrix}=\begin{pmatrix}1&0&0&0\\0&1&0&0\\0&0&0&1\\0&0&1&0\end{pmatrix}$$
$$=(Z_{+}I)ECR_{\downarrow}(XS) \tag{A7}$$

while its reverse reads (**Figure A4**)

$$CNOT_{\uparrow}=(II+IZ+XI-XZ)/2=$$
$$\begin{pmatrix}1&0&0&0\\0&0&0&1\\0&0&1&0\\0&1&0&0\end{pmatrix}=(HH)CNOT_{\downarrow}(HH)$$
$$=(HH)ECR_{\downarrow}(SS)(Z_{-}H) \tag{A8}$$

Acknowledgements

The results have been created using IBM Quantum. The views expressed are those of the authors and do not reflect the official policy or position of the IBM Quantum team. The authors thank Jakub Tworzydło for advice, technical support, and discussions, Stanisław Sołtan for the discussion about frequency collisions, and Witold Bednorz for consultations on error analysis. T.R. gratefully acknowledges the funding support by the program "Excellence initiative research university" for the AGH University in Krakówas well as the ARTIQ project: UMO-2021/01/2/ST6/00004 and ARTIQ/0004/2021. The authors also thank Bartłomiej Zglinicki and Bednorz family for the support.

Conflict of Interest

The authors declare no conflict of interest.

Data Availability Statement

The data that support the findings of this study are openly available in zenodo at https://doi.org/10.5281/zenodo.13771265, reference number 13771265.

Keywords

bell inequalities, no-signaling, quantum computer

Received: December 3, 2024
Revised: February 7, 2025
Published online:

[1] A. Einstein, B. Podolsky, N. Rosen, *Phys. Rev.* **1935**, *47*, 777.
[2] J. S. Bell, *Phys. (Long Island City, N.Y.)* **1964**, *1*, 195.
[3] J. F. Clauser, M. A. Horne, A. Shimony, R. A. Holt, *Phys. Rev. Lett.* **1969**, *23*, 880.
[4] J. F. Clauser, M. A. Horne, *Phys. Rev. D* **1974**, *10*, 526.
[5] P. H. Eberhard, *Phys. Rev. A* **1993**, *47*, R747.
[6] A. Garg, N. D. Mermin, *Phys. Rev. D* **1987**, *35*, 3831.
[7] P. M. Pearle, *Phys. Rev. D* **1970**, *2*, 1418.
[8] E. Santos, *Phys. Rev. A* **1992**, *46*, 3646.
[9] J.-A. Larsson, *J. Phys. A* **2014**, *47*, 424003.
[10] A. Aspect, J. Dalibard, G. Roger, *Phys. Rev. Lett.* **1982**, *49*, 1804.
[11] G. Weihs, T. Jennewein, C. Simon, H. Weinfurter, A. Zeilinger, *Phys. Rev. Lett.* **1998**, *81*, 5039.
[12] W. Tittel, J. Brendel, H. Zbinden, N. Gisin, *Phys. Rev. Lett.* **1998**, *81*, 3563.
[13] T. Scheidl, R. Ursin, J. Kofler, S. Ramelow, X.-S. Ma, T. Herbst, L. Ratschbacher, A. Fedrizzi, N. K. Langford, T. Jennewein, A. Zeilinger, *Proc. Natl. Acad. Sci. USA* **2010**, *107*, 19708.
[14] J. Hofmann, M. Krug, N. Ortegel, L. Gérard, M. Weber, W. Rosenfeld, H. Weinfurter, *Science* **2012**, *337*, 72.
[15] M. A. Rowe, D. Kielpinski, V. Meyer, C. A. Sackett, W. M. Itano, C. Monroe, D. J. Wineland, *Nature* **2001**, *409*, 791.
[16] D. N. Matsukevich, P. Maunz, D. L. Moehring, S. Olmschenk, C. Monroe, *Phys. Rev. Lett.* **2008**, *100*, 150404.
[17] M. Ansmann, H. Wang, R. C. Bialczak, M. Hofheinz, E. Lucero, M. Neeley, A. D. O'Connell, D. Sank, M. Weides, J. Wenner, A. N. Cleland, J. M. Martinis, *Nature* **2009**, *461*, 504.
[18] M. Giustina, A. Mech, S. Ramelow, B. Wittmann, J. Kofler, J. Beyer, A. Lita, B. Calkins, T. Gerrits, S. W. Nam, R. Ursin, A. Zeilinger, *Nature* **2013**, *497*, 227.
[19] B. G. Christensen, K. T. McCusker, J. B. Altepeter, B. Calkins, T. Gerrits, A. E. Lita, A. Miller, L. K. Shalm, Y. Zhang, S. W. Nam, N. Brunner, C. C. W. Lim, N. Gisin, P. G. Kwiat, *Phys. Rev. Lett.* **2013**, *111*, 130406.
[20] J. Handsteiner, A. S. Friedman, D. Rauch, J. Gallicchio, B. Liu, H. Hosp, J. Kofler, D. Bricher, M. Fink, C. Leung, A. Mark, H. T. Nguyen, I. Sanders, F. Steinlechner, R. Ursin, S. Wengerowsky, A. H. Guth, D. I. Kaiser, T. Scheidl, A. Zeilinger, *Phys. Rev. Lett.* **2017**, *118*, 060401.
[21] D. Rauch, J. Handsteiner, A. Hochrainer, J. Gallicchio, A. S. Friedman, C. Leung, B. Liu, L. Bulla, S. Ecker, F. Steinlechner, R. Ursin, B. Hu, D. Leon, C. Benn, A. Ghedina, M. Cecconi, A. H. Guth, D. I. Kaiser, T. Scheidl, A. Zeilinger, *Phys. Rev. Lett.* **2018**, *121*, 080403.
[22] Y. Liu, X. Yuan, C. Wu, W. Zhang, J.-Y. Guan, J. Zhong, H. Li, M.-H. Li, C. Abellán, M. W. Mitchell, S.-C. Shi, J. Fan, L. You, Z. Wang, X. Ma, Q. Zhang, J.-W. Pan, *Phys. Rev. A* **2019**, *99*, 022115.
[23] A. Bednorz, *Phys. Rev. D* **2016**, *94*, 085032.
[24] R. F. Streater, A. S. Wightman, *PCT, spin and statistics, and all that*, Benjamin, New York **1964**.
[25] A. Bednorz, *Eur. Phys. J. C* **2013**, *73*, 2654.
[26] B. Hensen, H. Bernien, A. E. Dréau, A. Reiserer, N. Kalb, M. S. Blok, J. Ruitenberg, R. F. L. Vermeulen, R. N. Schouten, C. Abellán, W. Amaya, V. Pruneri, M. W. Mitchell, M. Markham, D. J. Twitchen, D. Elkouss, S. Wehner, T. H. Taminiau, R. Hanson, *Nature* **2015**, *526*, 682.
[27] L. K. Shalm, E. Meyer-Scott, B. G. Christensen, P. Bierhorst, M. A. Wayne, M. J. Stevens, T. Gerrits, S. Glancy, D. R. Hamel, M. S. Allman, K. J. Coakley, S. D. Dyer, C. Hodge, A. E. Lita, V. B. Verma, C. Lambrocco, E. Tortorici, A. L. Migdall, Y. Zhang, D. R. Kumor, W. H. Farr, F. Marsili, M. D. Shaw, J. A. Stern, C. Abellán, W. Amaya, V. Pruneri, T. Jennewein, M. W. Mitchell, P. G. Kwiat, J. C. Bienfang, et al., *Phys. Rev. Lett.* **2015**, *115*, 250402.
[28] M. Giustina, M. A. M. Versteegh, S. Wengerowsky, J. Handsteiner, A. Hochrainer, K. Phelan, F. Steinlechner, J. Kofler, J.-Å. Larsson, C. Abellán, W. Amaya, V. Pruneri, M. W. Mitchell, J. Beyer, T. Gerrits, A. E. Lita, L. K. Shalm, S. W. Nam, T. Scheidl, R. Ursin, B. Wittmann, A. Zeilinger, *Phys. Rev. Lett.* **2015**, *115*, 250401.
[29] W. Rosenfeld, D. Burchardt, R. Garthoff, K. Redeker, N. Ortegel, M. Rau, H. Weinfurter, *Phys. Rev. Lett.* **2017**, *119*, 010402.
[30] S. Storz, J. Schär, A. Kulikov, P. Magnard, P. Kurpiers, J. Lütolf, T. Walter, A. Copetudo, K. Reuer, A. Akin, J.-C. Besse, M. Gabureac, G. J. Norris, A. Rosario, F. Martin, J. Martinez, W. Amaya, M. W. Mitchell, C. Abellan, J.-D. Bancal, N. Sangouard, B. Royer, A. Blais, A. Wallraff, *Nature* **2023**, *617*, 265.
[31] M. Smania, M. Kleinmann, A. Cabello, M. Bourennane, *arXiv:1801.05739* **2018**.
[32] A. Bednorz, *Phys. Rev. A* **2017**, *95*, 042118.
[33] a) G. Adenier, A. Yu. Khrennkov, *Fortschr. Phys.* **2017**, *65*, 1600096; b) D. A. Graft, *Open Physics* **2017**, *15*, 586.
[34] The Big Bell Test Collaboration, *Nature* **2018**, *557*, 212.
[35] S. Sołtan, D. Dopierała, A. Bednorz, *Ann. Phys.* **2020**, *532*, 2000333.
[36] There is a typo in Ref. [30] in Table SVI, missing 0 after period in rows 2 and 4.
[37] S. Storz, A. Kulikov, J. D. Schär, V. Barizien, X. Valcarce, F. Berterottire, N. Sangouard, J.-D. Bancal, A. Wallraff, *arXiv:2408.01299* **2024**.
[38] M. J. W. Hall, *Phys. Rev. A* **2010**, *82*, 062117.
[39] Y.-C. Liang, Y. Zhang, *Entropy* **2019**, *21*, 185.
[40] T. De Angelis, E. Nagali, F. Sciarrino, F. De Martini, *Phys. Rev. Lett.* **2007**, *99*, 193601.
[41] B.-H. Liu, X.-M. Hu, J.-S. Chen, Y.-F. Huang, Y.-J. Han, C.-F. Li, G.-C. Guo, A. Cabello, *Phys. Rev. Lett.* **2016**, *117*, 220402.
[42] A. Peres, D. R. Terno, *Rev. Mod. Phys.* **2004**, *76*, 93.
[43] M. J. W. Hall, *Phys. Lett. A* **1987**, *125*, 89.
[44] P. H. Eberhard, R. R. Ross, *Foundations of Physics Letters* **1989**, *2*, 127.
[45] M. J. W. Hall, *Phys. Rev. A* **2024**, *110*, 022209.

[46] J. Koch, T. M. Yu, J. Gambetta, A. A. Houck, D. I. Schuster, J. Majer, A. Blais, M. H. Devoret, S. M. Girvin, R. J. Schoelkopf, *Phys. Rev. A* **2007**, *76*, 042319.
[47] J. M. Gambetta, J. M. Chow, M. Steffen, *npj Quantum Inf.* **2017**, *3*, 2.
[48] F. Motzoi, J. M. Gambetta, P. Rebentrost, F. K. Wilhelm, *Phys. Rev. Lett.* **2009**, *103*, 110501.
[49] J. M. Gambetta, F. Motzoi, S. T. Merkel, F. K. Wilhelm, *Phys. Rev. A* **2011**, *83*, 012308.
[50] M. Malekakhlagh, E. Magesan, D. C. McKay, *Phys. Rev. A* **2020**, *102*, 042605.
[51] E. Magesan, J. M. Gambetta, *Phys. Rev. A* **2020**, *101*, 052308.
[52] IBM Quantum Platform, quantum.ibm.com.
[53] https://qiskit.org/textbook.
[54] P. Krantz, M. Kjaergaard, F. Yan, T. P. Orlando, S. Gustavsson, W. D. Oliver, *Appl. Phys. Rev.* **2019**, *6*, 021318.
[55] T. Alexander, N. Kanazawa, D. J. Egger, L. Capelluto, C. J. Wood, A. Javadi-Abhari, D. C. McKay, *Quantum Sci. Technol.* **2020**, *5*, 044006.
[56] D. Alsina, I. Latorre, *Phys. Rev. A* **2016**, *94*, 012314.
[57] D. Garcia-Martin, G. Sierra, *J. Appl. Math. Phys.* **2018**, *6*, 1460.
[58] IBM Quantum Learning, Tutorial: CHSH Inequality, learning.quantum.ibm.com/tutorial/chsh-inequality
[59] J. Brody, R. Avram, *Phys. Teach.* **2023**, *61*, 218.
[60] M. Kupczyński, *Open Phys.* **2017**, *15*, 739.
[61] a) C. E. Bonferroni, Teoria statistica delle classi e calcolo delle probabilita, *Pubblicazioni del R Istituto Superiore di Scienze Economiche e Commerciali di Firenze* **1936**; b) O. J. Dunn, *Ann. Math. Statistics* **1959**, *30*, 192.
[62] L. Lyons, *Ann. Appl. Stat.* **2008**, *2*, 887.
[63] European Organization For Nuclear Research and Open AIRE, Zenodo, CERN, **2021**, https://doi.org/10.5281/zenodo.13771265.
[64] A. Ketterer, T. Wellens, *Phys. Rev. Appl.* **2023**, *20*, 034065.
[65] E. Weiss, M. Cech, S. Soltan, M. Koppenhöfer, M. Krebsbach, T. Wellens, D. Braun, *arXiv:2405.20828* **2024**.
[66] D. C. McKay, C. J. Wood, S. Sheldon, J. M. Chow, J. M. Gambetta, *Phys. Rev. A* **2017**, *96*, 022330.
[67] L. C. G. Govia, et al., *New J. Phys.* **2023**, *25*, 123016.